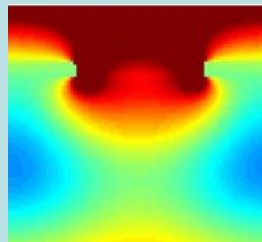
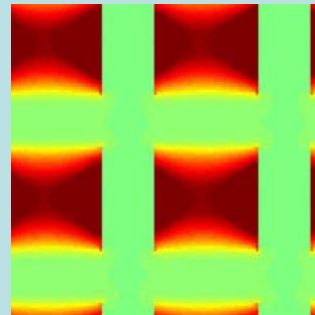
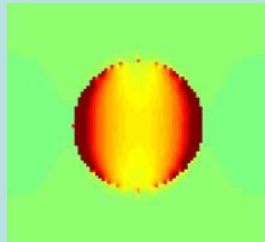


Photonic Micro- and Nano-Structures for Enhancing Infrared Detection

Shawn-Yu Lin
Wellfleet Constellation Chair Professor
Rensselaer Polytechnic Institute



Acknowledgement

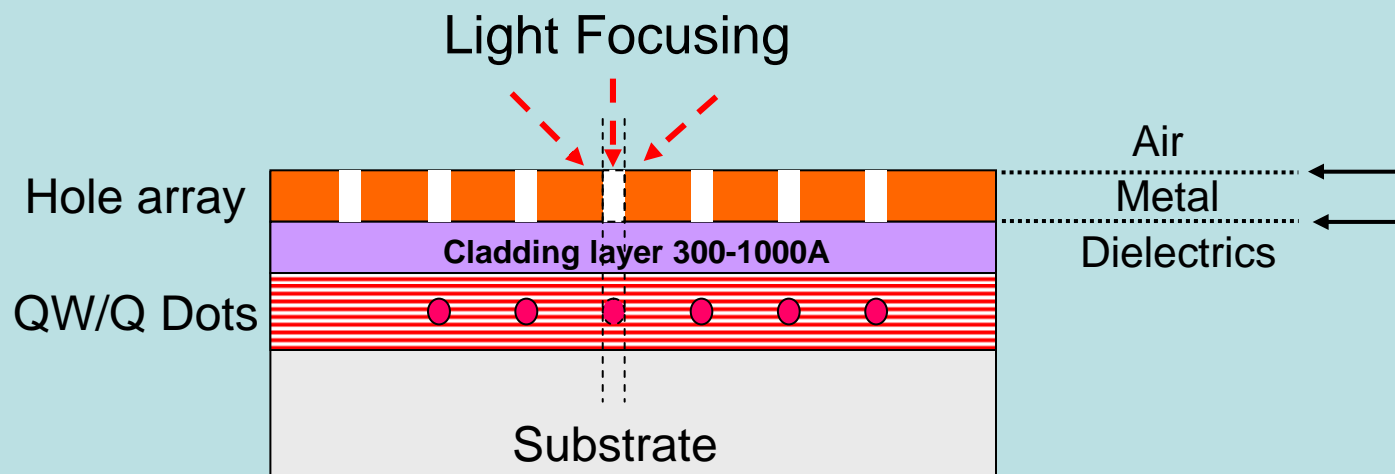
| | | |
|-----------------|-----------------|---------------|
| John Chang | Fabrication | RPI |
| Allan Chang | Fabrication | RPI |
| Min-Feng Chen | Calculation | RPI & NTU |
| Zu-Po Yang | Testing | RPI |
| James Bur | Testing | RPI |
| | | |
| Dan Huang | Theory & Design | AFRL-Kirtland |
| Dave Cardimona | Design & Appl. | AFRL-Kirtland |
| Sanjay Krishna | QD Growth | UNM |
| Yagya D. Sharma | QD Growth | UNM |

(This work is supported by AFOSR/ Dr. Gernot Pomrenke.)

Content

1. Introduction
2. Fabrication and Testing
3. FDTD simulation
4. Integration with a QDIP Detector
5. Other promising designs

Our Objective is to Achieve Light Focusing at Sub- λ at the Near Field Without Using a Conventional Lens.



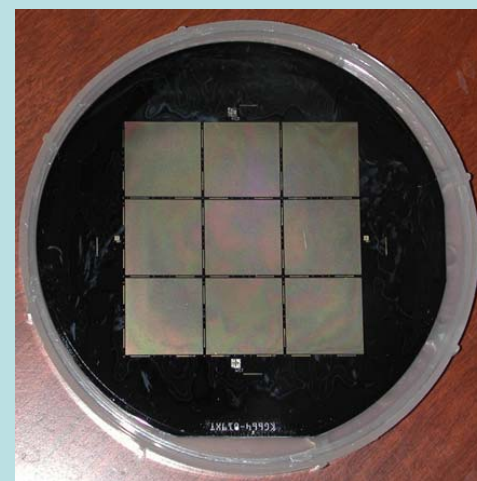
IR Sensing & Tracking

Objective

Field concentration at sub- λ
Compact / integrated design

Task

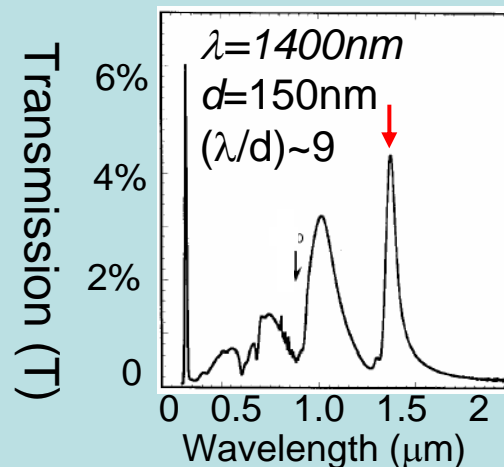
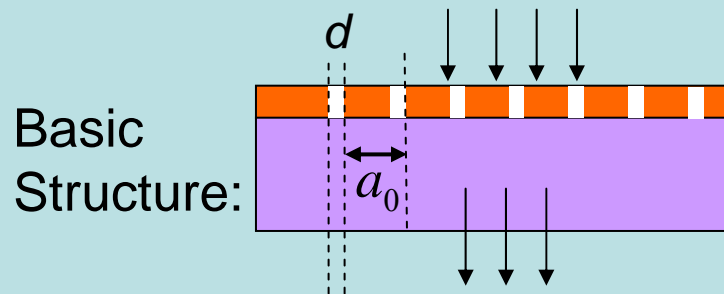
Maximize transmission (T)
Minimize area (A)
Maximize Flux: $(T/A) > 200\%$



Chip Processing

Most of The Research of Light Focusing at Sub- λ , $(\lambda/d) \gg 2$, is Focused On The Visible and Near-Infrared.

Extraordinary transmission through a 2D array
(Ebbesen et al, **Nature** 391, p.668, 1998)



$\lambda=1400\text{nm} \rightarrow$ **mid- and long- IR**

T: 2-5% \rightarrow **50-80%**

Flux: \rightarrow **200-400%**

Mechanism:

Surface plasma ($\omega_{sp} - k$)

Coupled interaction (tunneling)

A Brief Summary of Some of the Representative Works on 2D Hole Array

| | |  | | |  | | Figure-of-Merit | | |
|------------------------|--------|---|-------------|-------------|---|-----------------|--------------------|-------------------------|----------------|
| | Metal | λ | d | a_o | t | $\Delta\lambda$ | $(\lambda/d)^{**}$ | $\Delta\lambda/\lambda$ | T |
| Nature* '98 | Ag | 1.4 μ m | 150nm | 0.9 μ m | 200nm | 100nm | 9 | 0.08 | 5% |
| JOSA-B* '99 | Cr | 1.4 μ m | 0.5 μ m | 1 μ m | 100nm | 800nm | 2.8 | 0.6 | 40% |
| APL* '00 | Ag, Ni | 900nm | 400nm | 750nm | 300nm | 200nm | 2.2 | 0.25 | 43% |
| PRL* '01 | Ag | 800nm | 280nm | 750nm | 320nm | 150nm | 2.8 | 0.2 | 14% |
| JAP (aperiodic) '06 | Au | 700nm | 350nm | 1 μ m | 120nm | 80nm | 2 | 0.1 | 40% |
| | | | | | | | | | |
| This work | Au | 7.5μm | 1.3 μ m | 2.5 μ m | 50nm | 800nm | 6 | 0.1 | >60% |

- Trade-off (λ/d) and T

*reprint by all or part of the list: Ebbesen, Lezec, Ghaemi, Thio, Wolf, Pendry, etc

** $(\lambda/d)>2-3$: beyond the waveguide cutoff transmission.

Sample Fabrication and Optical Testing

Key Facilities At Rensselaer Micro-Clean-Room (MCR)



EVG Aligner and Bonder



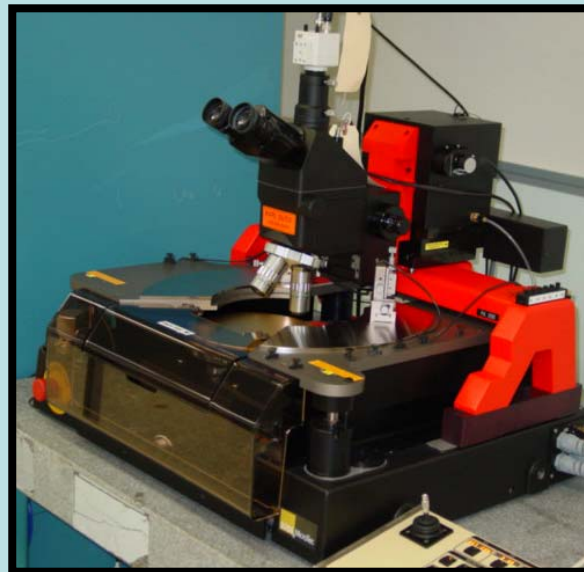
GCA Stepper



Temescal EBeam



IPEC/Westtech CMP



Suss Probe Station

CNF Cornell NanoScale
Science and Technology Facility

Rensselaer's Nano-Fabrication Facilities

EVG
NanoImprint



Adixen DRIE



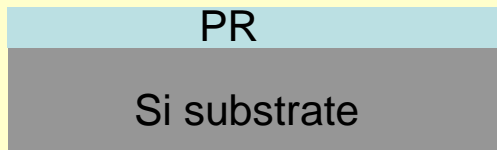
Applied PECVD



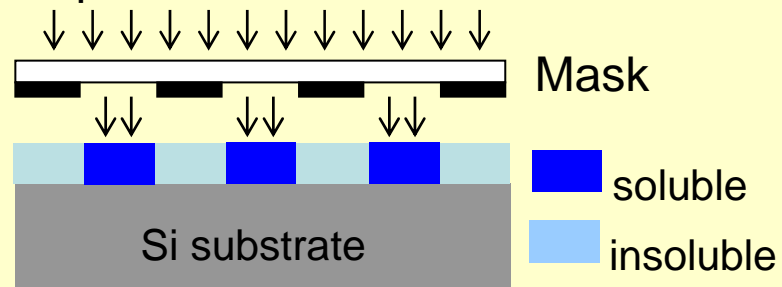
Zeiss SEM / EBeam

Process Flow For Fabricating 2D Hole Metallic Array.

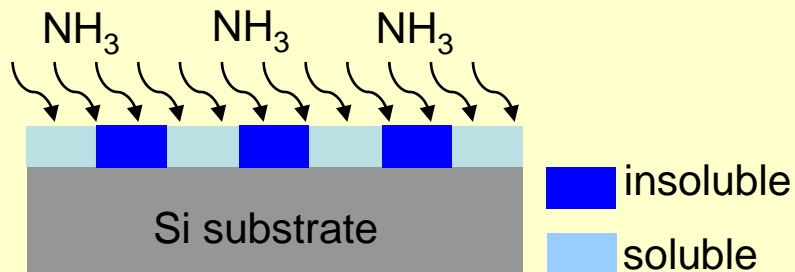
(I) Resist Spin-coating



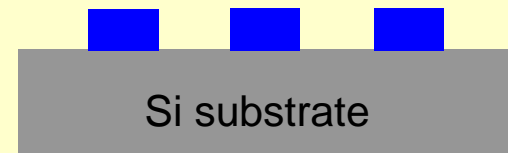
(II) Exposure



(III) NH₃ bake / Flood Exposure



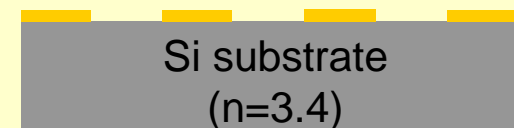
(IV) Developing



(V) Metal Evaporation ($t=50-200\text{nm}$)



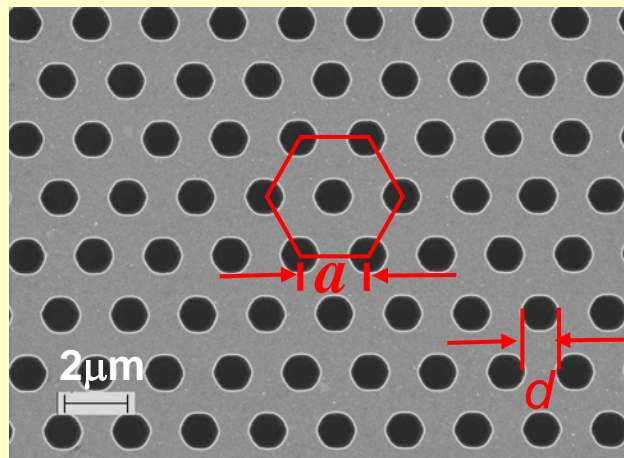
(VI) Lift-off



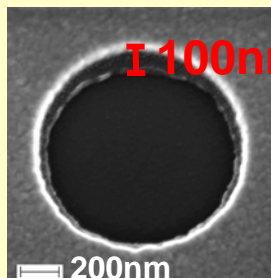
(Minimum feature size: $d=0.5-2\mu\text{m}$)

The SEM Image Shows Perfect Round Holes and Uniform Au Deposition.

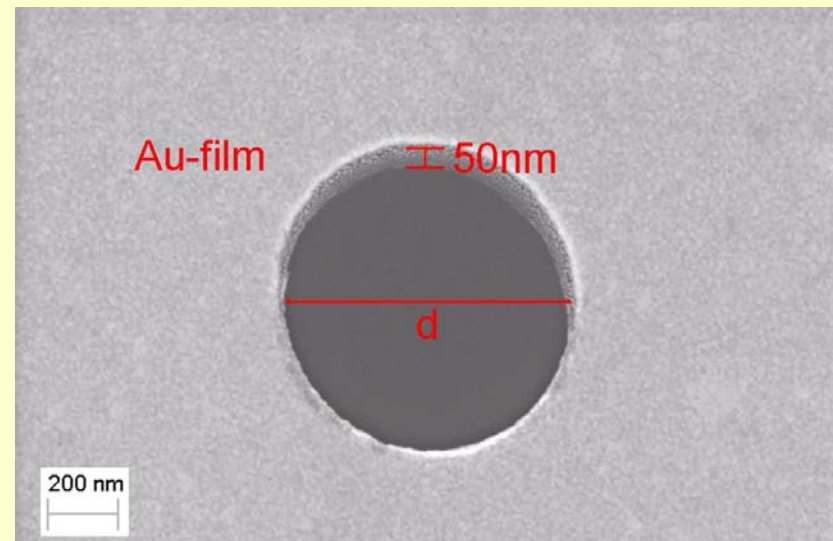
2D Au Hole-Array Sample



Au-film



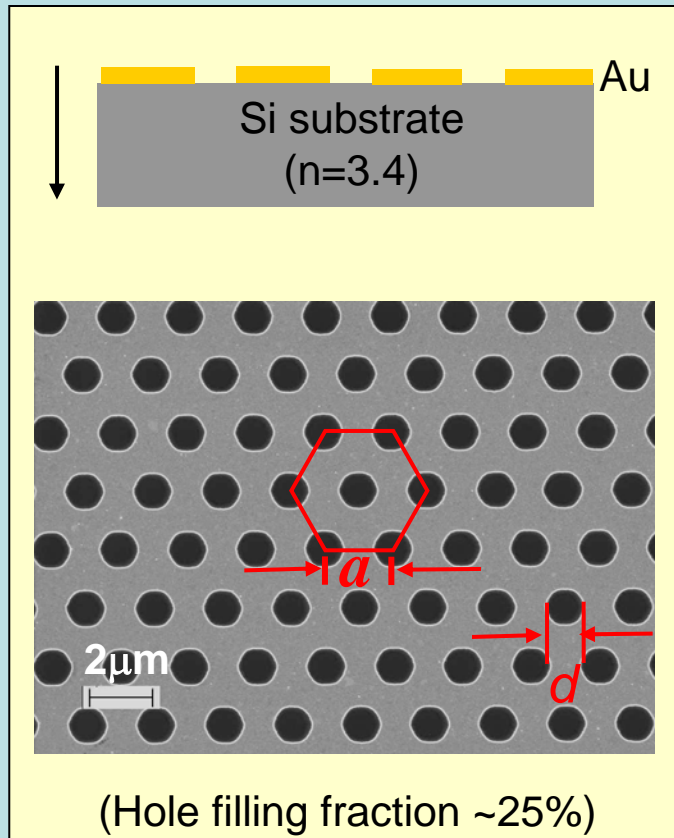
(Hole filling fraction ~25%)



$d = 1.3\mu\text{m}$

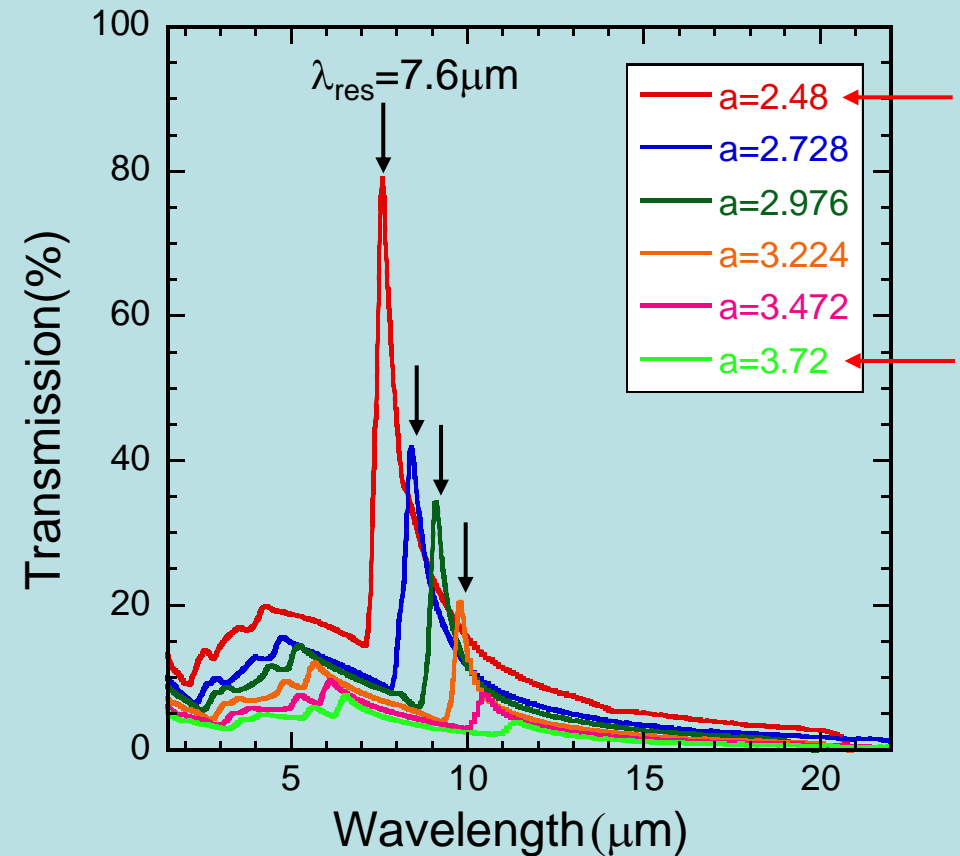
$t = 50\text{nm}$

A Clear, Sharp Transmission Peak Is Observed In The Infrared Wavelength.



Sample Parameters:

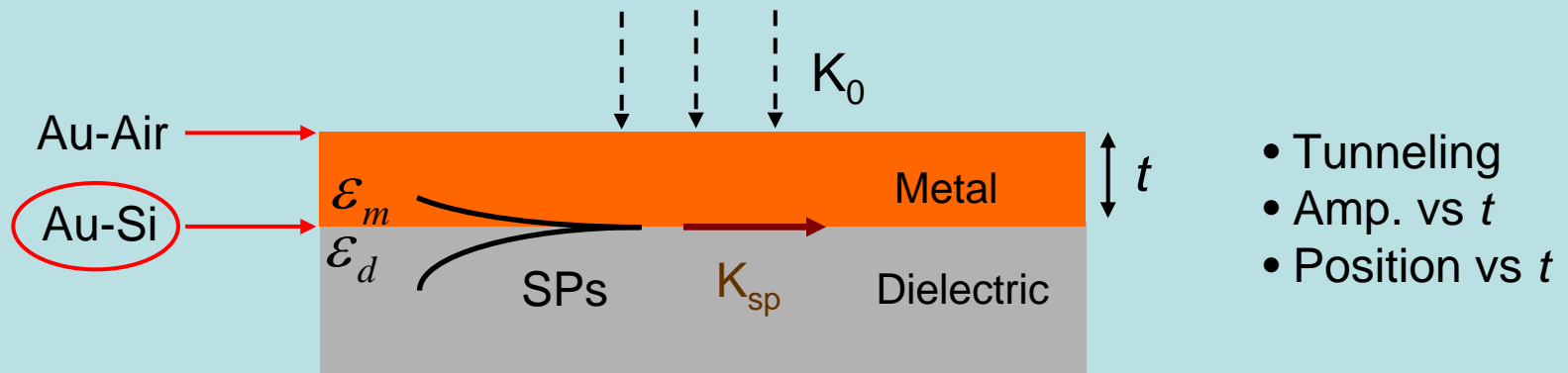
$a=2.48-3.72 \mu\text{m}$, $d=1.3\mu\text{m}$, $t=50\text{nm}$



- Infrared (sharp resonance)
- High T (T/A>300%)
- Sharp Resonance (vs “a” linearly)
- Lineshape asymmetry (Fano)

(*Work to be submitted for journal publication.)

The Sharp Transmission Is Due to Plasmonic Resonance at the Au-Silicon Interface.



In-Plane Momentum Matching

$$\vec{K}_{sp} = \vec{K}_{//} + (i\vec{G}_x + j\vec{G}_y)$$

$$\lambda_{sp}(i,j) = \frac{a}{\sqrt{i^2 + j^2}} \sqrt{\frac{\epsilon_m \epsilon_d}{\epsilon_m + \epsilon_d}}$$

$$\lambda_{sp}(i,j) = \frac{a}{\sqrt{\frac{4}{3}(i^2 + ij + j^2)}} \sqrt{\frac{\epsilon_m \epsilon_d}{\epsilon_m + \epsilon_d}}$$

λ_{sp} at the Au/Si Interface

| a (μm) | Calculated λ_{sp} (μm) | FDTD λ_{sp} (μm) | Measured λ_{sp} (μm) |
|-----------------------|---|---------------------------------------|---|
| 2.48 | 7.35 | 7.56 | 7.58 |
| 2.73 | 8.1 | 8.3 | 8.4 |
| 2.98 | 8.8 | 9 | 9.1 |
| 3.22 | 9.5 | 9.7 | 9.8 |
| 3.47 | 10.3 | 10.4 | 10.5 |
| 3.72 | 11 | 11.1 | 11.4 |

Our Structure Is Promising in Enhancing Transmission Flux (i.e. Transmission Amplitude / F.F.) to Much Greater Than 100%.

Table 1. Summary of sample geometries and measured transmission results, where a is lattice constant, d is hole diameter, t is thickness, F.F. is filling fraction, λ_{\max} is the wavelength of maximal transmission, T is transmission.

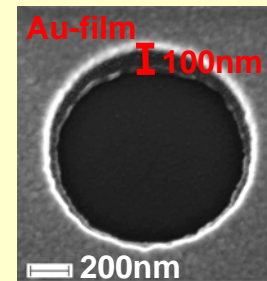
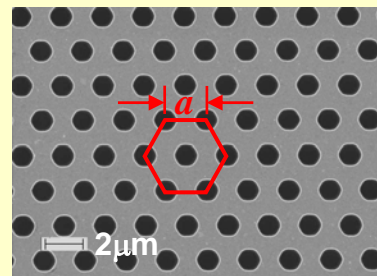
| Sample | a (μm) | d (μm) | t (nm) | F.F.(%) | λ_{\max} (μm) | T (%) | $T/\text{F.F.}$ |
|--------|-----------------------|-----------------------|----------|---------|------------------------------------|---------|-----------------|
| 1 | 2.480 | 1.3 | 50 | 24.90 | 7.58 | 79 | 3.17 |
| 2 | 2.728 | 1.3 | 50 | 20.58 | 8.40 | 42 | 2.04 |
| 3 | 2.976 | 1.3 | 50 | 17.29 | 9.12 | 34 | 1.97 |
| 4 | 3.224 | 1.3 | 50 | 14.73 | 9.82 | 20 | 1.36 |
| 5 | 3.472 | 1.3 | 50 | 12.70 | 10.46 | 7.7 | 0.61 |
| 6 | 3.720 | 1.3 | 50 | 11.06 | 11.37 | 3.9 | 0.35 |

Finite Difference Time Domain (FDTD) Simulation

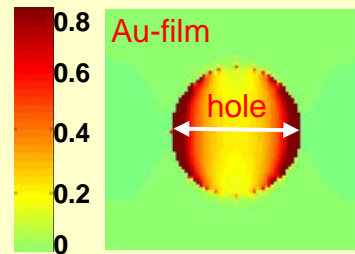
- Mode @ Au-Silicon Interface
- Origin of Field Concentration

(1) Results of FDTD Shows That The Fields Are Strongly Concentrated Near the Au-Air and Au-Si Interface.

SEM
Images

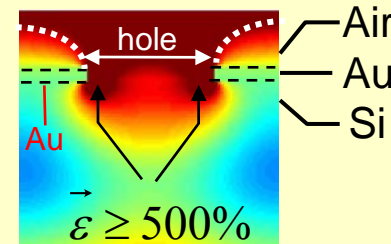


Top View



Field Concentration at
the Au-Air interface.

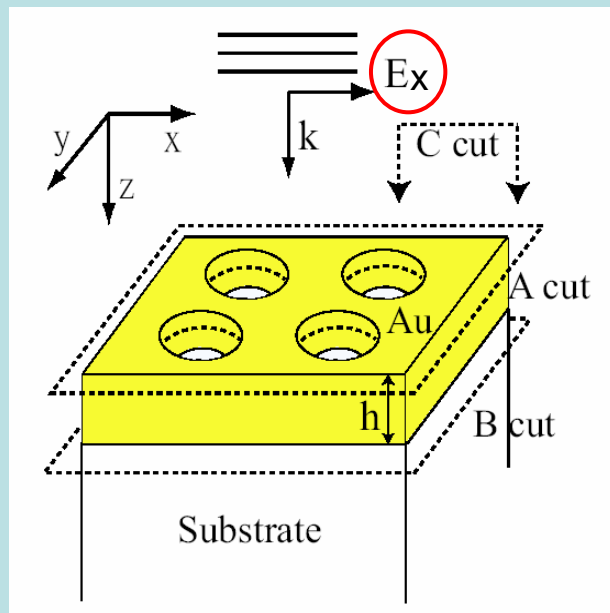
Side View



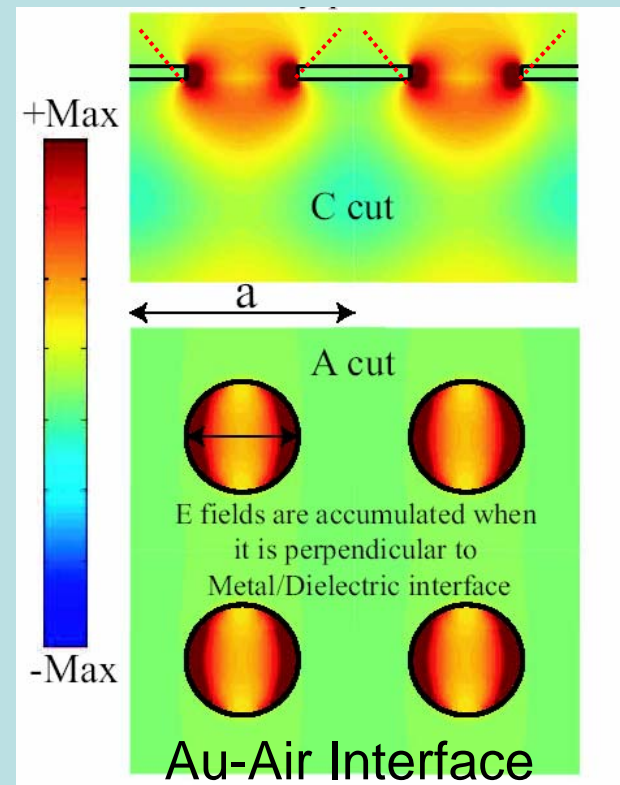
The EM field is funneled
around the metal corner.

- Au-Silicon resonance
- Light bends at the “corner”
- Focusing w/o lens, QD/QW/PV

(2) Results of FDTD Shows That The Fields Are Strongly Concentrated Near the Au-Air and Au-Si Interface.



(E_x Profile)



FDTD Summary

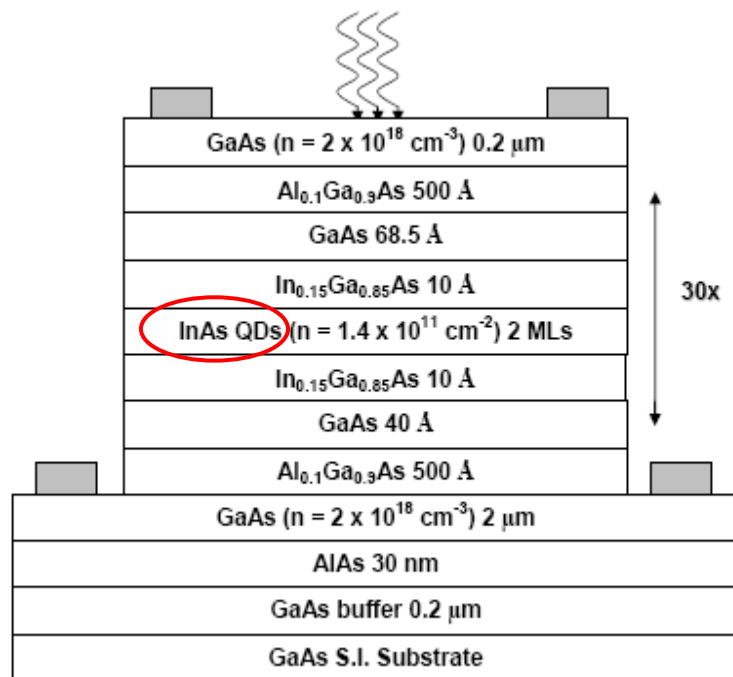
- Field concentration is induced at the metal corners.
- The resonance occurs at the Au-Si interface
- The 2D mode propagates along x with a wavevector, $k_{sp}=G$.

Integration with a QDIP Detector

- • Quantum Dot Sample Growth (UNM)
- • Sample Processing (RPI)
 - Testing

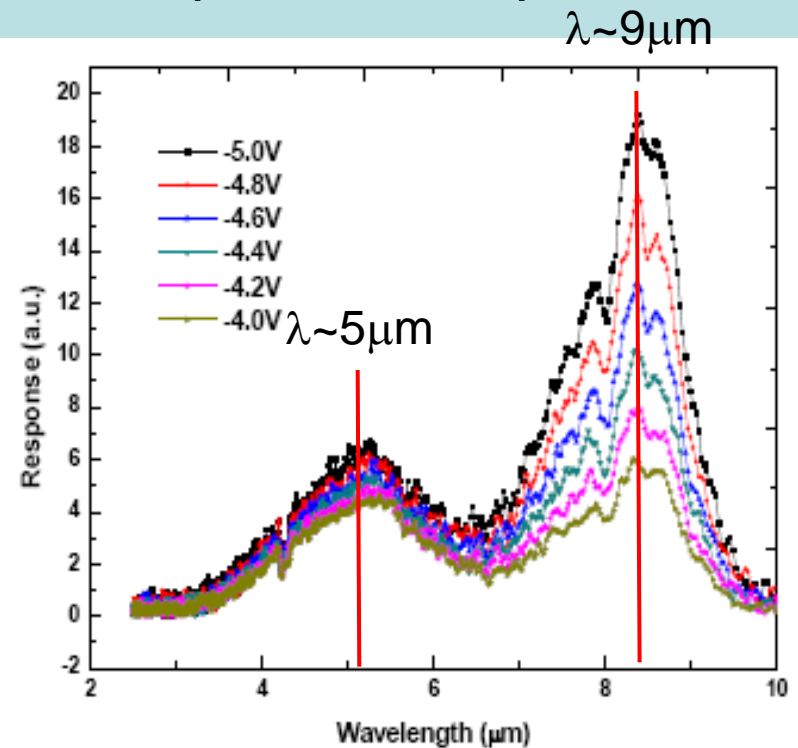
A High Quality QD Infrared Photodetector Sample With a Dual Band Response Was Grown at U New Mexico.

Sample Structure



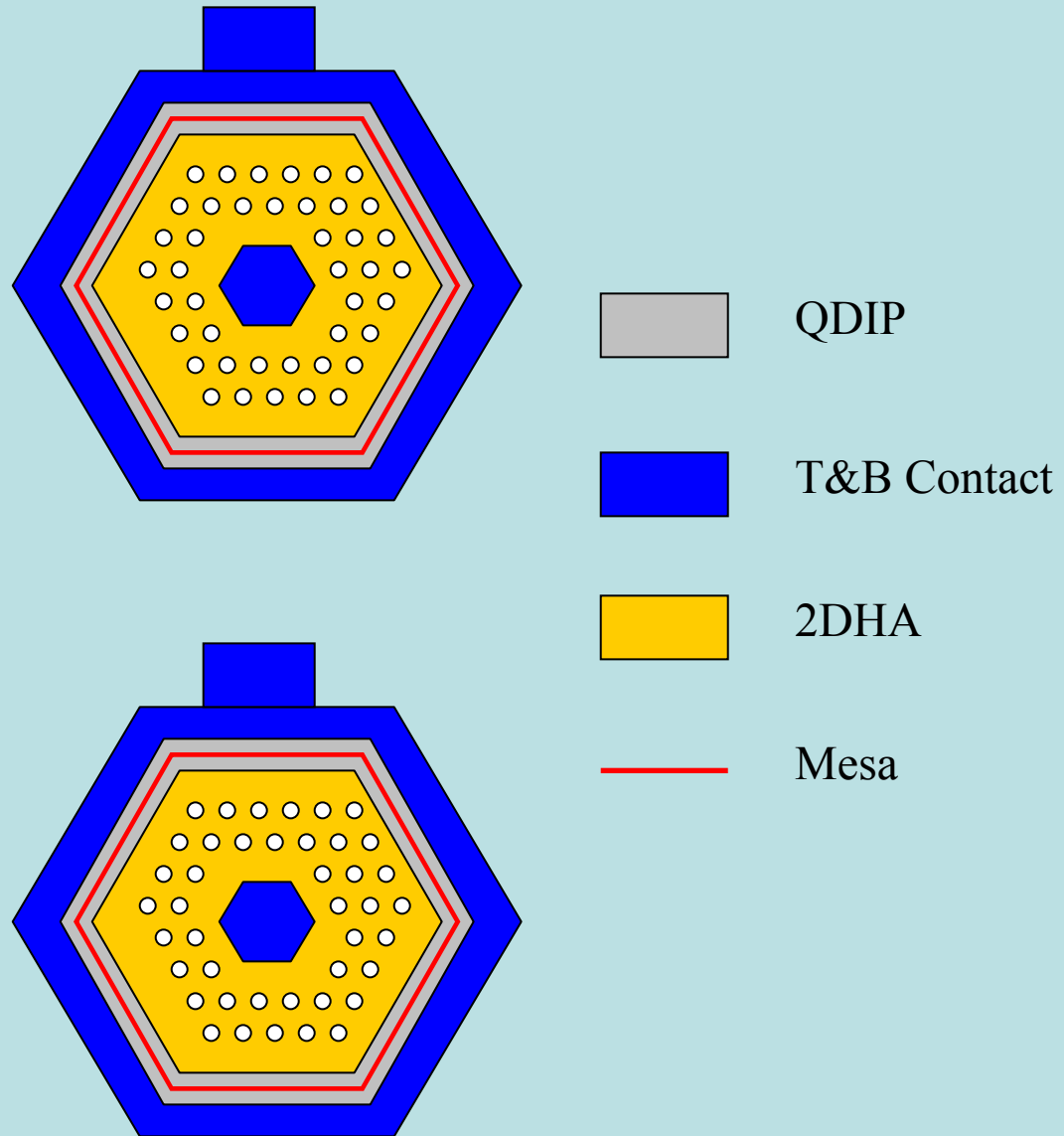
30 Periods Quantum Dot (QD)

Spectral Response

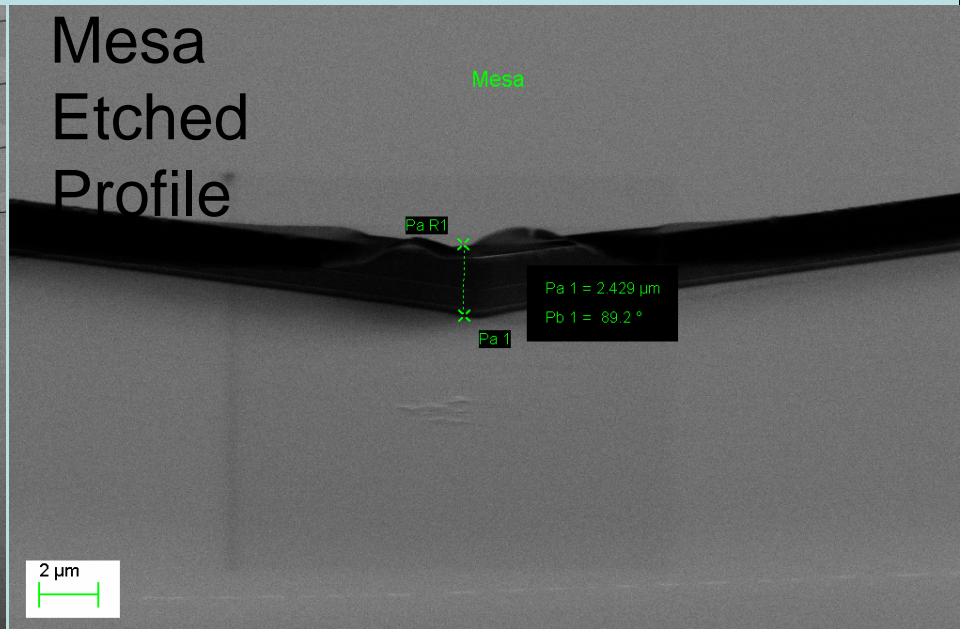
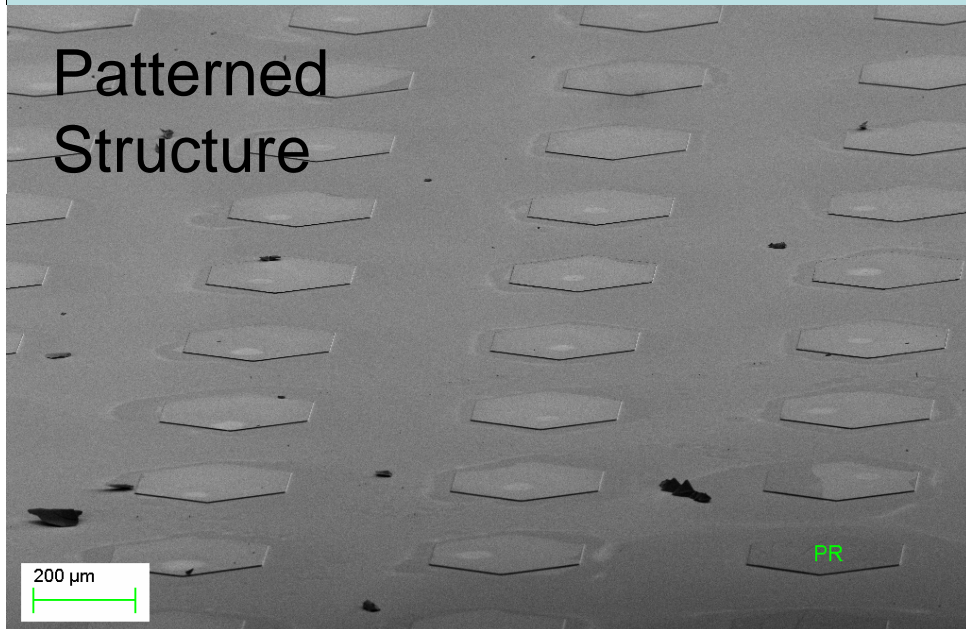
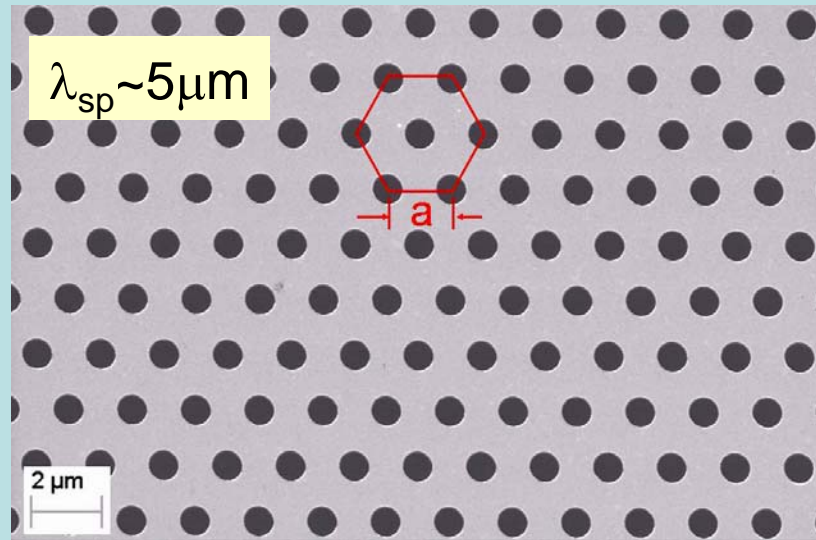


Spectral response for the QD infrared photodetector at 77K.

Mask Layout For Enhancing Infrared Response at $\lambda=5\mu\text{m}$ and $8.5\mu\text{m}$ Wavelengths.



Our Process Development Is Almost Complete For 2DHA and QDIP Integration .



Conclusion

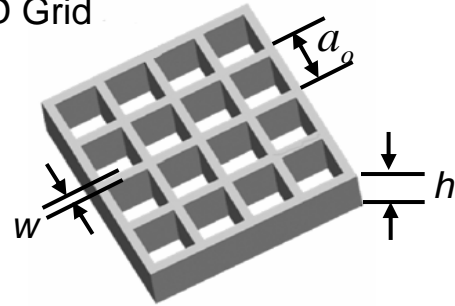
- Extended 2DHA focusing to the infrared ($\lambda=3-10\mu\text{m}$).
- Demonstrated a flux enhancement ($>300\%$) at sub- λ .
- Discovered the role of metal corner for light focusing.
- Integrate 2DHA with a QD infrared photodetector.

Appendix: Other Designs for Field Enhancement

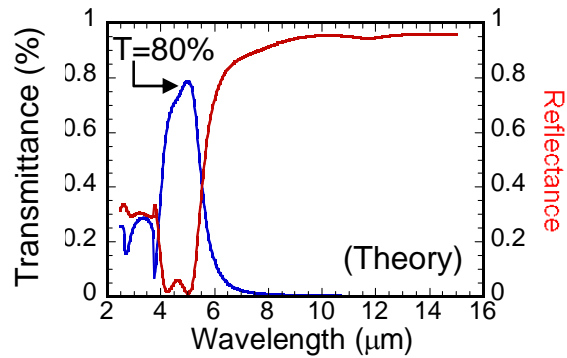
1. 2D metallic mesh design
2. 3D metallic photonic crystal

1. 2D Metallic Mesh Design

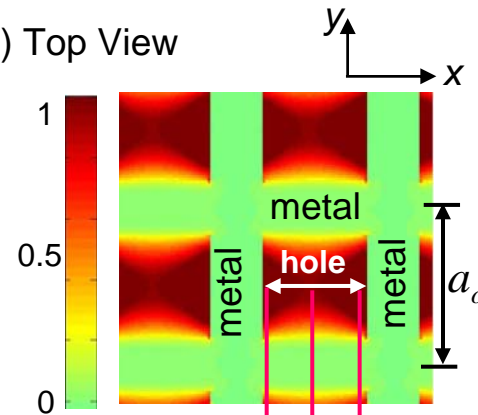
(a) 2D Grid



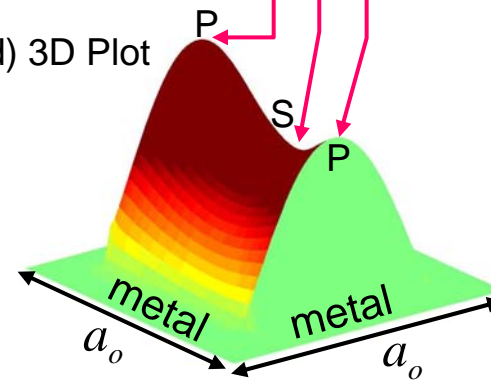
(b)



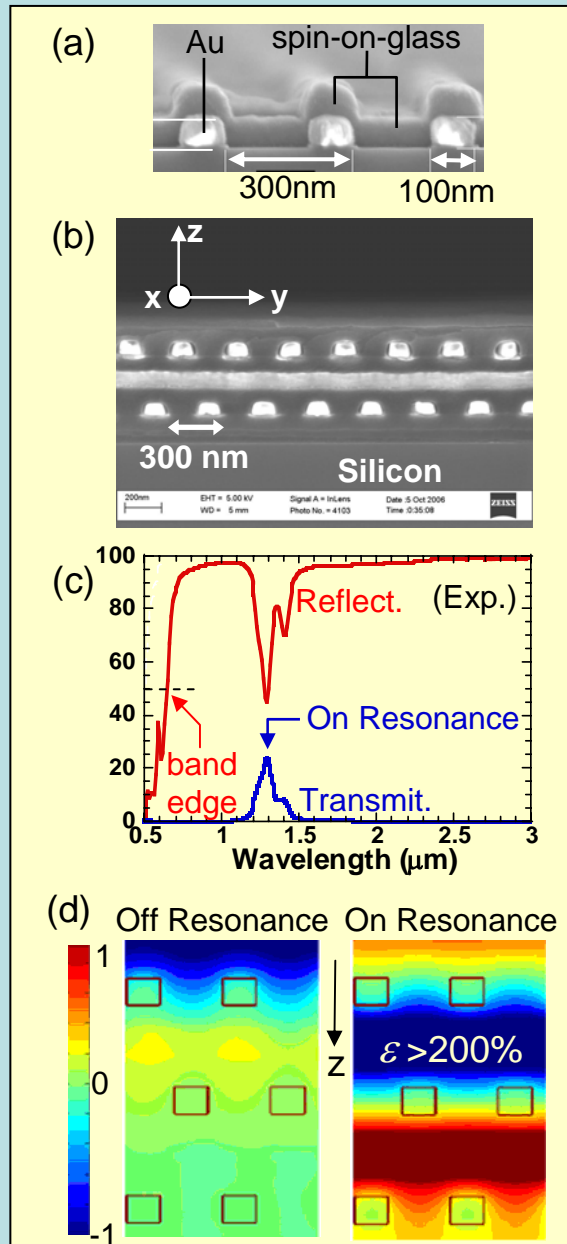
(c) Top View



(d) 3D Plot



2. 3D Metallic Photonic Crystal at Visible Wavelengths.



This 3D photonic-crystal has the shortest operating wavelength in the world. Its feature size is the smallest ever been produced in such a multi-layer nanostructure.

An experimental reflectance data taken at different incident angles. The band edge is at $\lambda \sim 650\text{nm}$.

The EM field is strongly enhanced, $>200\%$, when excited at the resonant frequency

(Optics Express **15**, 8428 (2007).)